Cycloadditions of 16-Electron 1,3-Dipoles with Ethylene. A Density Functional and CCSD(T) Study

Ming-Der Su,*,† Hsin-Yi Liao,† Wen-Sheng Chung,*,‡ and San-Yan Chu*,†

*Department of Chemistry, National Tsing Hua University, Hsinchu 30043, Taiwan, ROC, and
Department of Applied Chemistry, National Chiao Tung University, Hsinchu 30050, Taiwan, ROC*

The 1,3-dipolar cycloaddition (DC) reactions of ethylene with nitrile ylide (**CNC**), nitrile imine (**CNN**), nitrile oxide (**CNO**), diazomethane (**NNC**), azine (**NNN**), and nitrous oxide (**NNO**) in the gas phase were examined using the density functional theory and CCSD(T) calculations. All of the structures, including the precursor complexes and the transition structures, were completely optimized at the B3LYP/6-31G* level with single-point energies evaluated at CCSD(T)/6-311G**. The theoretical results suggest that the activation energies for the DC reactions of nitrile-type molecules (**CNC**, **CNN**, and **CNO**) are small (5.1−11 kcal/mol) and these reactions are very exothermic (−77 to −46 kcal/mol). In contrast, the DC reactions of **NNC**, **NNN**, and **NNO** are less exothermic (−39 to −6.0 kcal/mol) and have larger activation barriers (13−29 kcal/mol). Moreover, this work shows that the configuration mixing (CM) model based on Pross and Shaik's theory can successfully predict the relative ordering of the activation energy and reaction enthalpies of DC reactions. Combining our theoretical calculations and the CM model, the following conclusion emerges: a 16-electron 1,3-dipole reactant with more electropositive substituents at the terminal positions will possess a smaller singlet−triplet splitting. This will facilitate cycloaddition with the dipolarophile and will result in a larger exothermicity.

I. Introduction

1,3-Dipolar cycloaddition is the union of a 1,3-dipole with a multiple bond system (a dipolarophile) to form a five-membered ring. The process is remarkably useful and is regarded as one of the most general methods for the synthesis of five-membered heterocycles. Its versatility in the synthesis of heterocycles is comparable to that of the Diels−Alder reaction in the formation of carbocyclic systems. It is therefore not surprising that, during the last several decades, much experimental and theoretical work has been devoted to the study of the bonding nature and energy sequence of such cycloadditions.[1−33]

The 1,3-dipole is a triad of atoms (a−b−c) that has a π system of four electrons and can be represented by a zwitterionic octet resonance structure.[2−10] The compounds display electrophilic and nucleophilic reactivity. Each molecule has at least one resonance structure that shows a separation of charge in a 1,3-relationship.[3] The great majority of these compounds are isoelectronic with either 16- (such as nitrous oxide) or 18-valence-electron (such as ozone) compounds.[1] If all three atoms of the

† National Tsing Hua University.

‡ National Chiao Tung University.

(1) Perhaps the most outstanding contribution has come from the brilliant work of Rolf Huisgen. His efforts have helped transform the 1,3-dipolar addition from an almost obscure phenomenon into a major reaction type. See: (a) Huisgen, R. *Angew. Chem., Int. Ed. Engl.* **1963,** *2,* 562; (b) **1963,** *2,* 633.

(2) (a) Woodward, R. B.; Hoffmann, R. *Angew. Chem., Int. Ed. Engl.* **1969,** *8,* 781; (b) **1969,** *8,* 817.

(3) Carey, F. A.; Sundberg, R. J. In *Advance in Organic Chemistry, Part B*; Plenum Publ. Corp.: New York, 1977; p 212.

(4) Fukui, K. In *Molecular Orbitals in Chemistry, Physics and Biology*; Lowdin, P. O., Pullman, B., Eds.; Academic Press: New York, 1964.

(5) Fleming, I. In *Frontier Molecular Orbitals and Organic Chemical Reactions*; Wiley and Sons: New York, 1976.

(6) Huisgen, R. In *1,3-Dipolar Cycloaddition Chemistry*; Padwa, A., Ed.; John Wiley & Sons: New York, 1984; Vol. 1.

(7) Houk, K. N. *J. Am. Chem. Soc.* **1972,** *94,* 8953.

(8) Houk, K. N.; Sims, J. *J. Am. Chem. Soc.* **1973,** *95,* 3798.

(9) Houk, K. N.; Sims, J.; Duke, R. E., Jr.; Strozier, R. W.; George, J. K. *J. Am. Chem. Soc.* **1973,** *95,* 7287.

(10) Houk, K. N.; Sims, J.; Watts, C. R.; Luskus, T. J. *J. Am. Chem. Soc.* **1973,** *95,* 7301.

(11) Houk, K. N. *Acc. Chem. Res.* **1975,** *8,* 361.

(12) Poppinger, D. *J. Am. Chem. Soc.* **1975,** *97,* 7486.

(13) Caramella, P.; Houk, K. N.; Domelsmith, L. N. *J. Am. Chem. Soc.* **1977,** *99,* 4511.

(14) Dewar, M. J. S.; Olivella, S.; Rzepa, H. S. *J. Am. Chem. Soc.* **1978,** *100,* 5650.

(15) Komornicki, A.; Goddard, J. D.; Schaefer, H. F. *J. Am. Chem. Soc.* **1980,** *102,* 1763.

(16) Hiberty, P. C.; Ohanessian, G.; Schlegel, H. B. *J. Am. Chem. Soc.* **1983,** *105,* 719.

(17) Samuilov, Y. D.; Konovalov, A. I. *Russ. Chem. Rev.* **1984,** *53,* 332.

(18) Houk, K. N.; Firestone, R. A.; Munchausen, L. L.; Mueller, P. H.; Arison, B. H.; Garcia, L. A. *J. Am. Chem. Soc.* **1985,** *107,* 7227.

(19) Huisgen, R.; Mloston, G.; Langhals, E. *J. Am. Chem. Soc.* **1986,** *108,* 6401.

(20) Huisgen, R.; Mloston, G.; Langhals, E. *J. Org. Chem.* **1986,** *51,* 4085.

(21) McDouall, J. J. W.; Robb, M. A.; Niazi, U.; Bernardi, F.; Schlegel, H. B. *J. Am. Chem. Soc.* **1987,** *109,* 4642.

(22) Huisgen, R.; Langhal, E. *Tetrahedron Lett.* **1989,** *30,* 5369.

(23) Mloston, G.; Langhal, E.; Huisgen, R. *Tetrahedron Lett.* **1989,** *30,* 5373.

(24) Sosa, C.; Andzelm, J.; Lee, C.; Blake, J. F.; Chenard, B. L.; Butler, T. W. *Int. J. Quantum Chem.* **1994,** *49,* 511,

(25) Houk, K. N.; Gonzalez, J.; Li, Y. *Acc. Chem. Res.* **1995,** *28,* 81 and reference therein.

(26) Huisgen, R.; Fisera, L.; Giera, H.; Sustmann, R. *J. Am. Chem. Soc.* **1995,** *117,* 9671.

(27) Houk, K. N.; Wiest, O. *Top. Curr. Chem.* **1996,** *183,* 1.

(28) (a) Chung, W.-S.; Tsai, T.-L.; Ho, C.-C.; Chiang, M. Y. N.; le Noble, W. J. *J. Org. Chem.* **1997,** *62,* 4672. (b) Tsai, T.-L.; Chen, W.-C.; Yu, C.-H.; le Noble, W. J.; Chung, W.-S. *J. Org. Chem.* **1999,** *64,* 1099.

(29) Sustmann, R.; Sicking, W.; Huisgen, R. *J. Am. Chem. Soc.* **1995,** *117,* 9679.

(30) Sustmann, R.; Sicking, W.; Huisgen, R. *J. Org. Chem.* **1993,** *58,* 82.

(31) Huisgen, R.; Li, X. *Tetrahedron Lett.* **1983,** *24,* 4185.

(32) Mloston, G.; Huisgen, R. *Tetrahedron Lett.* **1989,** *30,* 7045.

(33) Huisgen, R.; Langhal, E.; Mloston, G.; Oshima, T. *Heterocycles* **1989,** *29,* 2069.

Table 1. 16-Electron 1,3-Dipoles with Resonance Structures

1,3-dipoles	resonance structures	abbreviation
Nitrile Ylide	$\overset{+}{HC}=\overset{-}{N}-\overset{-}{CH_2} \leftrightarrow HC\equiv\overset{+}{N}-\overset{-}{CH_2}$	CNC
Nitrile Imine	$\overset{+}{HC}=\overset{-}{N}-\overset{-}{NH} \leftrightarrow HC\equiv\overset{+}{N}-\overset{-}{NH}$	CNN
Nitrile Oxide	$\overset{+}{HC}=\overset{-}{N}-\overset{-}{O} \leftrightarrow HC\equiv\overset{+}{N}-\overset{-}{O}$	CNO
Diazomethane	$\overset{+}{N}=\overset{-}{N}-\overset{-}{CH_2} \leftrightarrow N=\overset{+}{N}-\overset{-}{CH_2}$	NNC
Azide	$\overset{+}{N}=\overset{-}{N}-\overset{-}{NH} \leftrightarrow N=\overset{+}{N}-\overset{-}{NH}$	NNN
Nitrous Oxide	$\overset{+}{N}=\overset{-}{N}-\overset{-}{O} \leftrightarrow N\equiv\overset{+}{N}-\overset{-}{O}$	NNO

dipole belong to the first row, a total of 18 different species, six of the 16-electron kind and twelve of the 18-electron kind, are possible.[9] The two all-octet resonance forms of the 16-electron 1,3-dipoles are shown in Table 1. On the other hand, dipolarophiles (d=e) are usually olefins or acetylenes, but other multiple bonds, such as the C=N bond of imines and the C=S bond of thioformaldehyde, also can act as dipolarophiles.[28-33]

The reactivity and regioselectivity of 1,3-dipolar cycloadditions have been discussed in terms of their frontier orbitals.[2-10] Most of the features may be understood on the basis of simple Hückel molecular orbital (HMO) theory. Although theoretical work presented by several research groups is quite exhaustive, we believe that a somewhat different approach and some new aspects emphasized here may supplement their results. The configuration mixing (CM) model[34,35] has been found to provide a powerful but simple method to understanding a variety of cycloadditions, and it appeared to us that the CM model would provide the key to the understanding of reactivity in 1,3-dipolar cycloadditions. This work confirms that conviction.

In recent years, the methods based on the density functional theory (DFT) have emerged as an alternative to traditional ab initio methods in the study of structure and reactivity of chemical systems.[36] In this study we report a theoretical investigation of 1,3-dipolar gas-phase cycloadditions using DFT calculations. The systems we choose to investigate here are the addition of ethylene to nitrile ylide (**CNC**), nitrile imine (**CNN**), nitrile oxide (**CNO**), diazomethane (**NNC**), azine (**NNN**), and nitrous oxide (**NNO**). They are listed in Table 1.

The present work will consider the following problems: (i) both the energy and structure of the orientation complex, if it exists, and the transition state of the reaction; (ii) a detailed understanding of the energetics and kinetics with regard to cycloaddition of the 1,3-dipoles; (iii) the effect of substituent electronegativity on the reactivity; and (iv) the factors that control the activation barrier for such 1,3-dipolar cycloadditions. It is found that the reactivity of the 16-electron dipole is strongly correlated to its singlet−triplet splitting. That

is to say, a knowledge of the singlet−triplet splitting of the 16-electron dipole species is of great importance in understanding its reactivity and reaction enthalpy because it can affect the driving force for cycloadditions. To the best of our knowledge, this is the first theoretical report concerning a systematic study of 1,3-dipolar cycloadditions based on the more sophisticated theory.

II. Calculation Methods

The geometries of reactants, orientation complexes, transition states, and products have been optimized using the hybrid density functional B3LYP method, i.e., Becke's three-parameter nonlocal-exchange functional[37] with the nonlocal correlation functional of Lee, Yang, and Parr,[38] with the 6-31G* basis set.[39] Vibrational frequencies, calculated at the B3LYP/6-31G* level, have been used for characterization of stationary points. All of the stationary points have been positively identified for minima (number of imaginary frequencies, NIMAG = 0) or transition states (NIMAG = 1).

To obtain more reliable energies, coupled cluster calculations with single and double excitations and a perturbative estimate of triple contributions (CCSD(T))[40] were carried out with the geometries optimized at the B3LYP/6-31G* level. These single-point CCSD(T) calculations were performed using the 6-311G**[41] basis set. Thus we denote these calculations as CCSD(T)/6-311G**//B3LYP/6-31G*. All of the DFT and CCSD(T) calculations were performed with the GAUSSIAN 94 package of programs.[42]

III. Geometries and Energetics of 1,3-Dipolar Cycloadditions

In this section the results for four regions on the potential energy surfaces will be presented: the reactants (16-electron dipole + C_2H_4; **Rea**), an orientation complex (**Ocx**),[43] the transition state (**TS**), and the cycloaddition product (**Pro**). The fully optimized geometries for those stationary points calculated at the B3LYP/6-31G* level are given in Figures 1−3, respectively. The corresponding total and relative energies at the DFT and CCSD(T) levels of theory are collected in Table 2. The potential energy profiles based on the CCSD(T) data in Table 2 are summarized in Figure 4. Several interesting results are found in these figures and in the table.

1
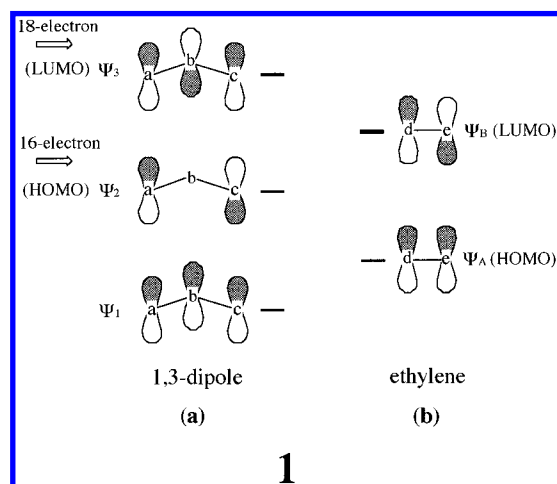
(34) (a) Shaik, S.; Schlegel, H. B.; Wolfe, S. In *Theoretical Aspects of Physical Organic Chemistry*; John Wiley & Sons Inc.: New York, 1992. (b) Pross, A. In *Theoretical and Physical Principles of Organic Reactivity*; John Wiley & Sons Inc.: New York, 1995.
(35) Su, M.-D. *Inorg. Chem.* **1995**, *34*, 3829.
(36) Ziegler, T. *Can. J. Chem.* **1995**, *73*, 743.

(37) (a) Becke, A. D. *J. Chem. Phys.* **1993**, *98*, 5648; (b) **1992**, *97*, 9173.
(38) Lee, C.; Yang, W.; Parr, R. G. *Phys. Rev.* **1988**, *B37*, 785.
(39) Hehre, W. J.; Ditchfield, R.; Pople, J. A. *J. Chem. Phys.* **1972**, *56*, 2257.
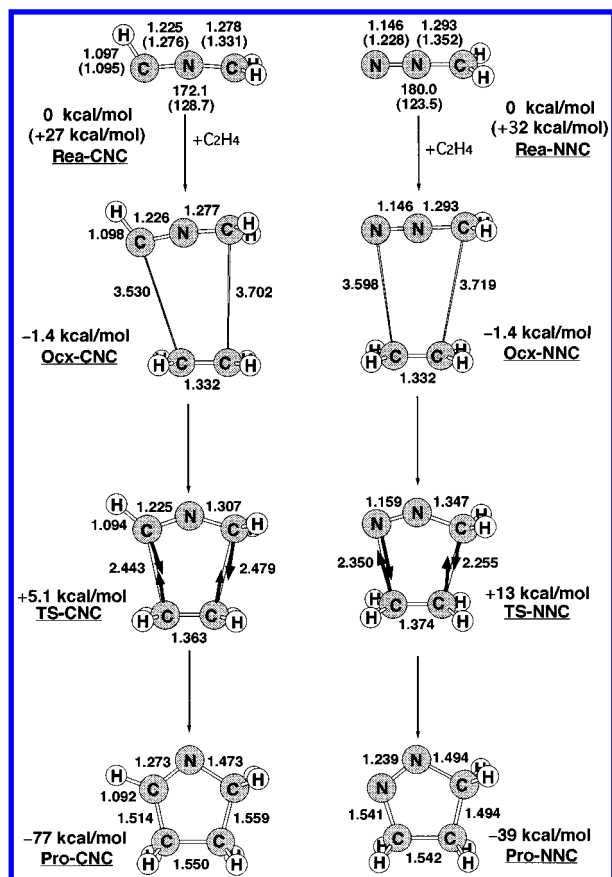
Figure 1. B3LYP/6-31G* optimized geometries (in Å and deg) of the reactants (singlet and triplet), precursor complex, transition state, and product of nitrile ylide (**CNC**) and diazoalkane (**NNC**). Values in parentheses are at the triplet state. The heavy arrows indicate the main atomic motions in the transition state eigenvector.
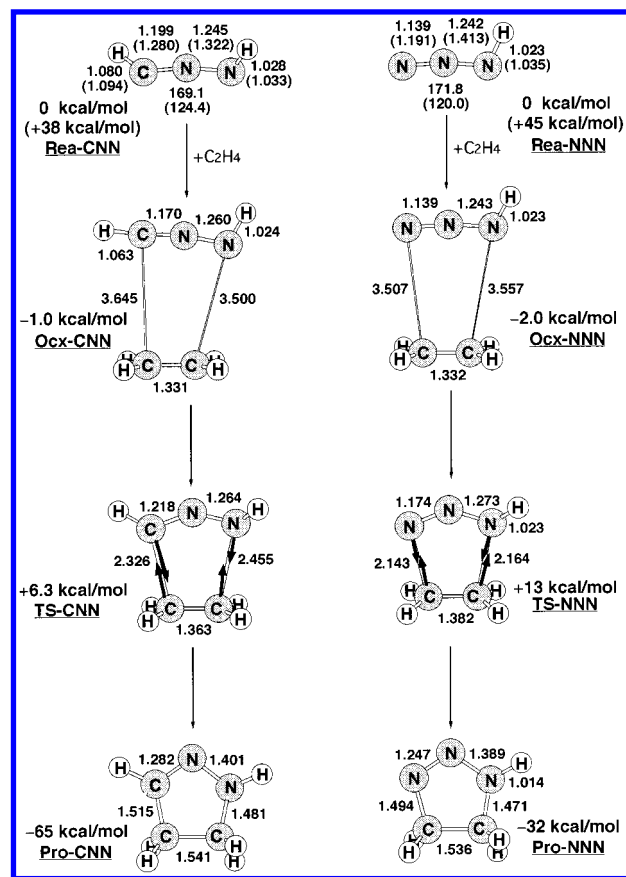
Figure 2. B3LYP/6-31G* optimized geometries (in Å and deg) of the reactants (singlet and triplet), precursor complex, transition state, and product of nitrile imine (**CNN**) and azine (**NNN**). Values in parentheses are at the triplet state. The heavy arrows indicate the main atomic motions in the transition state eigenvector.

First, a general outline of the valence molecular orbitals (MOs) in 1,3-dipoles has been given previously and needs no additional comments.[2,4,5,10] Basically, all 1,3-dipoles have in common a three atomic orbital π system containing four electrons analogous to an allyl anion (a–b–c), which can interact with an olefin in a six-electron transition state, energetically favored according to the Woodward–Hoffmann rules.[2] The main relevant π MOs between the two fragments, the 16-electron dipole and ethylene, are shown in **1**. It is clear from **1(a)** that in the triplet state, one electron is situated in the LUMO, in which antibonding interactions exist between the center and the terminal atoms, while a bonding interactions exists between the two terminal atoms. The bond distances r(a–b) and r(c–b) are therefore expected to be

longer, and the bond angle ∠a–b–c is expected to be smaller for the triplet compared to the singlet. This prediction agrees qualitatively with our B3LYP/6-31G* results for all cases as given in Figures 1–3.

Moreover, reactants **CNC–Rea**, **NNC–Rea**, **CNN–Rea**, **NNN–Rea**, **CNO–Rea**, and **NNO–Rea** have been calculated both as low-spin (singlet) and as high-spin (triplet) compounds. As expected, our DFT and CCSD-(T) calculations indicate that they all possess a singlet ground state. As seen in Table 2, our theoretical findings suggest that the 16-electron dipoles with a more electronegative atom in the terminal position show a substantial stabilization of the singlet state over the triplet and thus higher separations are obtained. For instance, the CCSD(T)/6-311G**//B3LYP/6-31G* calculations show an increasing trend in the singlet–triplet splitting for **CNC–Rea** (27.2 kcal/mol) < **CNN–Rea** (38.1 kcal/mol) < **CNO–Rea** (64.4 kcal/mol) and for **NNC–Rea** (32.0 kcal/mol) < **NNN–Rea** (45.3 kcal/mol) < **NNO–Rea** (55.6 kcal/mol) (Table 3). We shall use the above results to explain the origin of barrier heights for their cycloadditions in a later section.

Second, the geometries and energies of complexation of the 1,3-dipole with ethylene, i.e., **CNC–Ocx**, **NNC–Ocx**, **CNN–Ocx**, **NNN–Ocx**, **CNO–Ocx**, and **NNO–Ocx**, were also calculated. The optimized geometries are shown in Figures 1–3. For convenience, the energies are given relative to the reactant molecules, i.e., 1,3-dipole + C_2H_4, which are also summarized in Table 2.

(40) Lee, T. J.; Scuseria, G. In *Quantum Mechanical Electronic Structure Calculations with Chemical Accuracy*; Langnoff, S. F., Ed.; Kluwer Academic Press: Dordrecht, The Netherlands, 1995.

(41) Krishnan, R.; Binkley, J. S.; Seger, R.; Pople, J. A. *J. Chem. Phys.* **1980**, *72*, 650.

(42) *Gaussian 94*; Frisch, M. J.; Trucks, G. W.; Schlegel, H. B.; Gill, P. M. W.; Johnson, B. G.; Robb, M. A.; Cheeseman, J. R.; Keith, T.; Petersson, G. A.; Montgomery, J. A.; Raghavachari, K.; Al-Laham, M. A.; Zakrzewski, V. G.; Ortiz, J. V.; Foresman, J. B.; Cioslowski, J.; Stefanov, B. B.; Nanayakkara, A.; Challacombe, M.; Peng, C. Y.; Ayala, P. Y.; Chen, W.; Wong, M. W.; Andres, J. L.; Replogle, E. S.; Gomperts, R.; Martin, R. L.; Fox, D. J.; Binkley, J. S.; Defrees, D. J.; Baker, J.; Stewart, J. P.; Head-Gordon, M.; Gonzalez, C.; Pople, J. A. Gaussian, Inc.: Pittsburgh, PA, 1995.

(43) In this work, we use the term *orientation complex* to characterize the spatial arrangement of the reactants at the beginning of the bonding interaction. See ref 1.
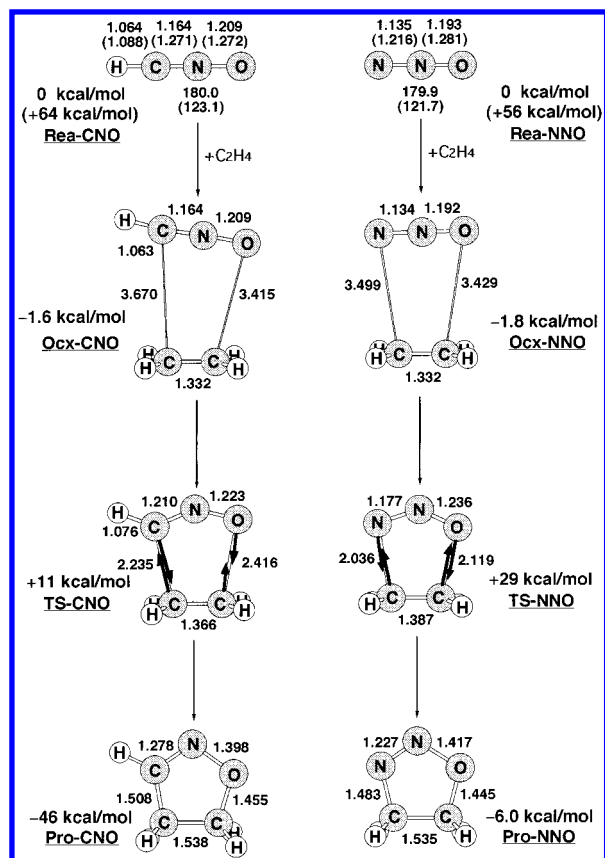
Figure 3. B3LYP/6-31G* optimized geometries (in Å and deg) of the reactants (singlet and triplet), precursor complex, transition state, and product of nitrile oxide (**CNO**) and nitrous oxide (**NNO**). Values in parentheses are at the triplet state. The heavy arrows indicate the main atomic motions in the transition state eigenvector.

Because the dipole plus ethylene reaction leads to a five-membered ring product as expected for a 1,3-dipolar cycloaddition, it is reasonable to assume a parallel plane approach of dipole to ethylene in the formation of the dipole–ethylene complex. As will be shown below, the parallel plane orientation of the reacting molecules is maintained along this reaction coordinate. Calculated vibrational frequencies for the orientation complexes reveal that these structures are true minima on the potential energy surface. Moreover, as one can see from Figures 1–3, the calculated bond distances for the dipole–olefin contacts (ca. 3.42–3.72 Å) are more than twice as long as those calculated for the corresponding products (ca. 1.50 Å). It is not surprising that such long bond distances are reflected in the calculated complexation energy. As shown in Table 2, the energy of the orientation complex relative to its corresponding reactants is less than 1.98 kcal/mol at the CCSD(T) level of theory. Accordingly, our theoretical calculations show that these complexes are weakly bound and fall in a shallow minimum at large distances on the reaction surface. In addition, because the dipole–ethylene distances in the transition state are calculated to be about 2.04–2.48 Å, the orientation complexes studied in the present work with dipole–ethylene distances of about 3.42–3.72 Å must fall on the reaction coordinate prior to the transition state. This suggest that they are precursors to the actual cycloaddition product, which means that the stereochemical properties of reaction including product formation will be influenced by the

stereochemistry of the π complex. Therefore, it is interesting to relate the geometry of the orientation complexes obtained in this work to the geometry of the transition states and the products of the cycloaddition reaction. As seen in Figures 1–3, compared to the structures of the isolated reactants, both 1,3-dipole and ethylene geometries in the orientation complexes are essentially unperturbed. Furthermore, because all of the complex binding energies are too low (ca. 1.03–1.98 kcal/mol at the CCSD(T) level of theory),[44] it seems that experimental detection of intermediates formed in the gas phase at room temperature is unlikely.[43]

Third, the optimized transition states (**CNC–TS, NNC–TS, CNN–TS, NNN–TS, CNO–TS,** and **NNO–TS**) along with the calculated transition vectors are shown in Figures 1–3, respectively. The arrows in the figures indicate the directions in which the atoms move in the normal coordinate corresponding to the imaginary frequency. It is apparent that these transition states connect the corresponding orientation complexes to the cycloaddition products. Examination of the single imaginary frequency for each transition state ($379i$ cm^{-1} for **CNC–TS**, $457i$ cm^{-1} for **NNC–TS**, $356i$ cm^{-1} for **CNN–TS**, $449i$ cm^{-1} for **NNN–TS**, $407i$ cm^{-1} for **CNO–TS**, and $465i$ cm^{-1} for **NNO–TS**) provides an excellent confirmation of the concept of the cycloaddition process. That is, the reactants approach each other with their molecular planes parallel, and two new bonds are formed at the same time. These reactions appear to be concerted; we have been able to locate only one TS for each reaction and have confirmed that it is a true TS on the basis of frequency analysis.

It should be pointed out that, although 1,3-dipolar cycloadditions were introduced more than 35 years ago, experimental studies have been unable to choose conclusively between the synchronous, concerted mechanism proposed by Huisgen[1,45] and the stepwise, diradical path favored by Firestone.[46] There are several reports of theoretical studies about both of these mechanisms of reaction.[12–16,21,25,27] Many of these calculations favor the concerted nature of the cycloaddition.[25] Though we have not carried out theoretical calculations on the diradical mechanism, the present DFT and CCSD(T) calculations on the six representative 1,3-dipolar cycloadditions imply that the concerted path is very promising.

A comparison of the six transition structures yields a number of trends. As seen in Figures 1–3, there is a dramatic effect on the intermolecular distances at the saddle points. Increasing the electronegativity of the terminal atoms in the dipole causes a large decrease in the dipole–ethylene distance. That is, the two newly forming bond lengths decreases in the order **CNC–TS** (2.44 Å, 2.48 Å) > **CNN–TS** (2.33 Å, 2.46 Å) > **CNO–TS** (2.24 Å, 2.42 Å), and **NNC–TS** (2.26 Å, 2.35 Å) > **NNN–TS** (2.14 Å, 2.16 Å) > **NNO–TS** (2.04 Å, 2.12 Å). It should be noted that the dipole–ethylene distances of

(44) Nevertheless, orientation complexes, as a result of van der Waals interactions, have recently been found for ozone and ethylene in the gas phase and were confirmed by ab initio calculations. See: (a) Gillies, C. W.; Gillies, J. Z.; Suenram, R. D.; Lovas, F. J.; Kraka, E.; Cremer, D. *J. Am. Chem. Soc.* **1991**, *113*, 2412. (b) Gillies, J. Z.; Gillies, C. W.; Lovas, F. J.; Matsumura, K.; Suenram, R. D.; Kraka, E.; Cremer, D. *J. Am. Chem. Soc.* **1991**, *113*, 6408.
(45) Huisgen, R. *J. Org. Chem.* **1976**, *41*, 403.
(46) (a) Firestone, R. A. *J. Org. Chem.* **1968**, *33*, 2285. (b) Firestone, R. A. *Tetrahedron* **1977**, *33*, 3009.

Table 2. Total Energies[a] and Relative Energies[b] Computed at the B3LYP/6-31G* and CCSD(T)/6-311G**//B3LYP/6-31G* Levels of Theory[c]

systems	B3LYP[d]				CCSD(T)[d]			
	Rea[e]	**Ocx**	**TS**	**Pro**	**Rea[f]**	**Ocx**	**TS**	**Pro**
CNC	−132.669 67	−211.257 76	−211.246 10	−211.372 09	−132.347 67	−210.733 70	−210.723 42	−210.853 66
	(0.0)	(−0.3968)	(+6.922)	(−72.14)	(0.0)	(−1.358)	(+5.093)	(−76.63)
CNN	−148.697 59	−227.285 25	−227.274 02	−227.384 74	−148.361 91	−226.747 41	−226.735 76	−226.849 19
	(0.0)	(−0.1286)	(+6.920)	(−62.56)	(0.0)	(−1.031)	(+6.281)	(−64.90)
CNO	−168.571 62	−247.160 05	−247.140 97	−247.232 17	−168.214 11	−246.600 51	−246.580 09	−246.670 77
	(0.0)	(−0.6153)	(+11.36)	(−45.87)	(0.0)	(−1.592)	(+11.22)	(−45.68)
NNC	−148.739 26	−227.327 28	−227.303 98	−227.385 72	−148.403 14	−226.789 22	−226.766 60	−226.849 92
	(0.0)	(−0.3539)	(+14.27)	(−37.03)	(0.0)	(−1.387)	(+12.81)	(−39.48)
NNN	−164.782 26	−243.370 46	−243.342 27	−243.411 45	−164.422 56	−242.809 57	−242.785 39	−242.857 11
	(0.0)	(−0.4690)	(+17.22)	(−26.19)	(0.0)	(−1.977)	(+13.20)	(−31.81)
NNO	−184.660 27	−263.249 27	−263.210 24	−263.264 82	−184.292 21	−262.678 91	−262.630 29	−262.685 56
	(0.0)	(−0.9643)	(+23.53)	(−10.73)	(0.0)	(−1.779)	(+28.74)	(−5.950)

[a] Values in atomic units. [b] Values in kcal/mol. [c] All optimized geometries can be found in Figures 1−3. [d] Values in the parentheses are the relative energies, corresponding to its reactants. [e] The B3LYP/6-31G* energy of ethylene is −78.587 46 au. [f] The CCSD(T)/6-311G**// B3LYP/6-31G* energy of ethylene is −78.383 86 au.
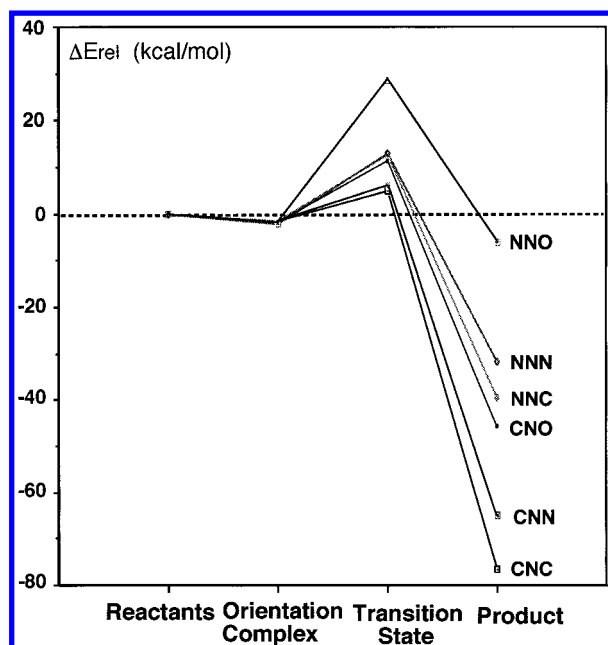

Figure 4. Potential energy surfaces for the cycloadditions of the 16-electron dipoles (**CNC**, **CNN**, **CNO**, **NNC**, **NNN**, and **NNO**) with ethylene. The relative energies are taken from the CCSD(T)/6-311G**//B3LYP/6-31G* values as given in Table 2. For optimized structures of the stationary points see Figures 1−3.

the nitrile-type reactions are longer than those of the azo-type ones; for example, **CNC−TS** > **NNC−TS**, **CNN−TS** > **NNN−TS**, and **CNO−TS** > **NNO−TS**. In addition, the DFT calculations suggest that, the C=C double bond is stretched by 2.4%, 2.4%, 2.6%, 3.2%, 3.8%, and 4.2% for **CNC−TS**, **CNN−TS**, and **CNO−TS**, **NNC−TS**, **NNN−TS**, and **NNO−TS**, respectively, relative to its value of ethylene (1.331 Å). All of these features strongly indicate that the transition structures for the dipoles with less electronegative atoms occupying the terminal positions take on more reactant-like character than the dipoles with more electronegative atoms lying on the terminal positions. Consequently, the barriers are encountered earlier in the cycloadditions of the former than of the later. As will be shown below, this is consistent with the Hammond postulate,[47] which associates an

(47) Hammond, G. S. *J. Am. Chem. Soc.* **1954**, 77, 334.

earlier transition state with a smaller barrier and a more exothermic reaction.

Furthermore, it is clearly seen that, for the 16-electron dipole, the more electronegative the atom lying in the terminal position, the higher the activation energy for the 1,3-dipolar cycloaddition. For instance, as demonstrated in Table 2 (CCSD(T) calculations), because the electronegativity order is C < N < O, the barrier height for the cycloaddition increases in the order **CNC−TS** (5.09 kcal/mol) < **CNN−TS** (6.28 kcal/mol) < **CNO−TS** (11.2 kcal/mol), and **NNC−TS** (12.8 kcal/mol) < **NNN−TS** (13.2 kcal/mol) < **NNO−TS** (28.7 kcal/mol). It is worth noting that the activation barriers for the nitrile-type reactions are smaller than those for the azo-type ones, namely, **CNC−TS** < **NNC−TS**, **CNN−TS** < **NNN−TS**, and **CNO−TS** < **NNO−TS**.

Fourth, the optimized product geometries (**CNC−Pro**, **NNC−Pro**, **CNN−Pro**, **NNN−Pro**, **CNO−Pro**, and **NNO−Pro**) are also collected in Figures 1−3, respectively. It should be noted that the two newly formed bonds in the transition structures are stretched on average by 60%, 60%, and 57% relative to their final equilibrium values in **CNC**, **CNN**, and **CNO** cycloadditions and 52%, 45%, and 42% for **NNC**, **NNN**, and **NNO** cycloaddition, respectively. Again, these features indicate that a dipole with less electronegative atoms in the terminal position reaches the transition state relatively early, whereas the dipole with more electronegative atoms in the terminal positions arrives at the transition state relatively late. Thus, one may anticipate a larger exothermicity for the former, which is confirmed by our CCSD(T) calculations. For instance, the order of exothermicity follows the same trend as the activation energy: **CNC−Pro** (−76.6 kcal/mol) < **CNN−Pro** (−64.9 kcal/mol) < **CNO−Pro** (−45.7 kcal/mol), and **NNC−Pro** (−39.5 kcal/mol) < **NNN−Pro** (−31.8 kcal/mol) < **NNO−Pro** (−5.95 kcal/mol). Note that the nitrile-type cycloadditions are more exothermic than the azo-type ones, i.e., **CNC−Pro** < **NNC−Pro**, **CNN−Pro** < **NNN−Pro**, and **CNO−Pro** < **NNO−Pro**.

Moreover, comparing the structures of the cycloaddition products and their corresponding isolated reactants, as shown in Figures 1−3, it is worth noting that the geometrical parameters of the dipole moiety in the product resemble more closely those of the triplet than those of the singlet 1,3-dipolar reactions. This strongly implies that the triplet 1,3-dipole takes part in the singlet

surface during the cycloaddition process. We shall explain this phenomenon in more detail in a later section.

IV. Origin of the Barrier and Reaction Enthalpy for 1,3-Dipolar Cycloadditions

All of the computational results can be rationalized using a simple valence bond model based upon reactant and product spin-coupling, which is denoted as the configuration mixing (CM) model.[34,35] In this model the total energy profile is decomposed into two component curves: one, associated with the reactant spin-coupling (reactant bonding situation), is denoted as the *reactant configuration*, and the other, associated with the product spin-coupling (product bonding situation), is denoted as the *product configuration*. Along the reaction coordinate, the behavior of the reactant configuration is repulsive and that of the product configuration is attractive. The crossing of the two curves defines the transition state and determines the energy barrier.

In Figure 5 we have represented the qualitative behavior of the two configurations for the addition of the 1,3-dipole to ethylene. The reactant configuration describes a situation where the two 2p π orbitals centered on C_a and C_c are singlet spin-coupled to form the π bond, while the two π electrons on the ethylene moiety are spin-paired to formed the olefin bond (reactant coupling) as illustrated in **2**. The product configuration corresponds to a situation where the electron pairs are coupled to allow both a−d and c−e bond formation (product coupling) as shown in **3**.

^{1}[a-b-c]^{1}[d=e]
reactant configuration
2

^{3}[a-b-c]^{3}[d=e]
product configuration
3
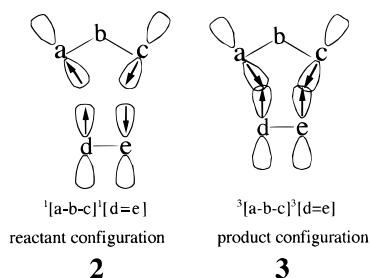
To obtain the product configuration **3** from the reactant configuration **2**, each of the two original electron pairs needs to be uncoupled. In other words, those two electron pairs require excitation from the singlet to the triplet state. Thus, the reactant and product configurations are labeled ^{1}[a−b−c]^{1}[d=e] and ^{3}[a−b−c]^{3}[d=e], respectively. It should be noted that ^{3}[a−b−c]^{3}[d=e] is an overall singlet configuration, despite the fact that it contains within it two local triplets. Consequently, it is the avoided crossing of these two configurations that leads to the simplest description of the ground-state energy profiles for the 1,3-dipolar cycloaddition.

This CM model shows that the barrier height ($\Delta E^{\ddagger}$) and the reaction enthalpy (ΔH) are strongly influenced by the combined effect of two factors: the singlet−triplet splitting for each of the reactants, i.e., ΔE_{st} (= $E_{triplet} - E_{singlet}$ for the 1,3-dipole) and $\Delta E_{\pi\pi^*}$ (= $E_{triplet} - E_{singlet}$ for ethylene). Accordingly, as demonstrated in Figure 5, if $\Delta E_{\pi\pi^*}$ is a constant, then a smaller value of ΔE_{st} is expected (i) to reduce the reaction barrier because the crossing of the reactant and product configurations is lower in energy, (ii) to produce a larger exothermicity because the energy of the product is now lower than that of the reactant, and (iii) to lead to an earlier transition
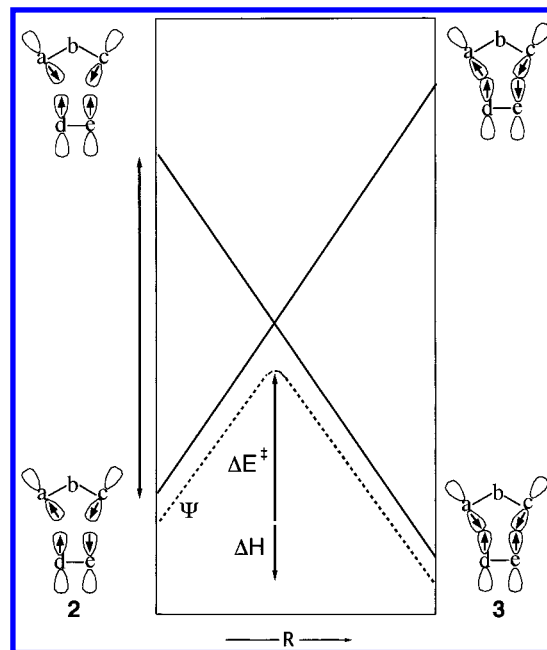

Figure 5. Energy diagram for an oxidative addition reaction showing the formation of a state curve (Ψ) by mixing two configurations: the reactant configuration (2) and the product configuration (3). It is apparent that both the activation energy ($\Delta E^{\ddagger}$) and reaction enthalpy (ΔH) is proportional to ΔE_{st} (= $E_{triplet} - E_{singlet}$ for the 16-electron dipole) and $\Delta E_{\pi\pi^*}$ (= $E_{triplet} - E_{singlet}$ for ethylene). See the text.

state because the crossing point is now earlier along the reaction coordinate. In short, the smaller the ΔE_{st} of the 1,3-dipole, the lower the barrier height, the earlier the transition state, and the larger the exothermicity.

Our model calculations confirm the above predictions. As shown in Table 3, the CCSD(T) calculations suggest an increasing trend in ΔE_{st} for **CNC−Rea** (27.2 kcal/mol) < **CNN−Rea** (38.1 kcal/mol) < **CNO−Rea** (64.4 kcal/mol), and **NNC−Rea** (32.0 kcal/mol) < **NNN−Rea** (45.3 kcal/mol) < **NNO−Rea** (55.6 kcal/mol). These results are in accordance with the trend in activation energy and enthalpy ($\Delta E^{\ddagger}$, ΔH) for 1,3-dipolar cycloadditions, which in kcal/mol are **CNC** (5.09, −76.6) < **CNN** (6.28, −64.9) < **CNO** (11.2, −45.7), and **NNC** (12.8, −39.5) < **NNN** (13.2, −31.8) < **NNO** (28.7, −5.95), respectively (Table 2). As a result, our theoretical findings are in excellent agreement with the CM model. This investigation provides strong evidence that the singlet−triplet splitting can be used as a guide to predict the reactivity of the 1,3-dipoles. Thus, to find a good model for the facile 1,3-dipolar cycloaddition, an understanding of the singlet−triplet splitting ΔE_{st} of the 16-electron dipoles is crucial.

Before further discussion, two points should be made. First, we have also examined the relationship between the HOMO−LUMO energy gaps and the activation barriers for the aforementioned six systems as shown in Table 3. It can be seen that only HOMO$_{dipole}$−LUMO$_{ethylene}$ energy gaps correlate with the increase in the insertion barriers.[48] Besides this, the singlet−triplet splitting ΔE_{st} of the dipoles is also directly associated with the activation energy and the enthalpy for the 1,3-dipolar cycloaddition. Second, as already shown in Figure 5, if a dipole

---

(48) This may be denoted as HOMO-controlled (the interaction of the dipole HOMO with the dipolarophile LUMO is greatest). See ref 10.

Table 3. HOMO and LUMO Energies,[a] Singlet−Triplet Energy Gaps,[b] Barriers,[b] and Enthalpies[b] for 1,3-Dipolar Cycloadditions[c]

system	HOMO	LUMO	$\Delta E_{\text{HO−LU}}$[d]	$\Delta E_{\text{LU−HO}}$[e]	ΔE_{st}[f]	$\Delta E^{\ddagger}$[g]	ΔH[h]
CNC	−0.3113	+0.1284	0.3301	0.3950	+27.19	+5.093	−76.63
CNN	−0.3479	+0.1152	0.3667	0.3818	+38.09	+6.281	−64.90
CNO	−0.4017	+0.1816	0.4205	0.4482	+64.39	+11.22	−45.68
NNC	−0.3257	+0.1346	0.3445	0.4012	+31.99	+12.81	−39.48
NNN	−0.3986	+0.1263	0.4174	0.3929	+45.32	+13.20	−31.81
NNO	−0.4885	+0.1477	0.5073	0.4143	+55.60	+28.74	−5.950

[a] Values in atomic units. [b] Values in kcal/mol. [c] All at the CCSD(T)/6-311G** level. [d] The energy difference between the HOMO of the 1,3-dipoles and the LUMO of the ethylene. The LUMO of reactant ethylene is 0.018 80 au. [e] The energy difference between the HOMO of ethylene and the LUMO of the 1,3-dipoles. The HOMO of reactant ethylene is −0.2666 au. [f] A positive value indicates a singlet ground state. [g] The activation energy of the transition state, relative to its corresponding reactants. [h] The exothermicity of the products, relative to its corresponding reactants (also see Table 2).

reactant has a singlet ground state with a low lying-triplet state, it may readily undergo a synchronous concerted reaction due to involvement of the triplet state in the reaction. The supporting evidence comes from the fact that the geometrical parameters of the final product should resemble those of the corresponding triplet reactants, rather than the singlet ones. This is exactly what we have seen in our DFT calculations as shown in Figures 1−3.

From the above analysis, one may wonder why the 16-electron dipoles with the less electronegative atom in the terminal position are more reactive than those with the more electronegative atom at the terminal positions. According to Su's work[49] based on the perturbation theory, see **1**, it was found that the HOMO (Ψ_2) of 1,3-dipoles increases in energy upon going from more electronegative substituents in the terminal positions to more electropositive substituents at the terminal positions. This would lead to the stabilization energy of the former being larger than that of the later. As a result, one might expect, for 16-valence-electron three-center systems, that the substitution of more electronegative atoms is most energetically favorable at the terminal positions. This conclusion is consistent with the experimentally known 16-valence-electron molecules, such as CCO, OCO, NNO, SCN−.[49] Moreover, the activation energy of such 1,3-dipolar cycloadditions is quite large, which is attributable to a low-lying HOMO, resulting in a larger singlet−triplet splitting (ΔE_{st}). Conversely, when the terminal atom (either a or c) in the 1,3-dipole (a−b−c) is replaced by a more electropositive atom, its HOMO (Ψ_2)−LUMO (Ψ_3) energy gap is reduced and this favors the high spin state, leading to a smaller ΔE_{st}. Consequently, with the above analysis in mind, one may then expect that the 16-electron 1,3-dipole reactant with more electropositive substituents at terminals will lead to a smaller singlet−triplet splitting ΔE_{st}, which in turn, will facilitate cycloaddition with the dipolarophile and will result in a larger exothermicity. This is exactly what we observed in the present work, as shown earlier.[50]

V. Conclusion

In this paper we have investigated the potential energy surfaces associated with the gas-phase reactions of 16-electron 1,3-dipoles with ethylene using both a B3LYP approach with the 6-31G* basis set and a CCSD(T) approach with the more accurate 6-311G** basis set. The comparison between the results obtained at the B3LYP and CCSD(T) levels indicates that a DFT computational approach with a basis set of double-ζ quantity plus polarization functions (6-31G*) can provide a reliable description for this class of reactions.[27] In particular, the performance of the B3LYP approach leads to energy barriers and reaction enthalpies which are not far from those obtained by the reliable but much more expensive CCSD(T) approach. Finally, we have demonstrated that the computational results can be rationalized using a simple diabatic model, i.e., the CM model. In the present case, the CM model indicates the singlet−triplet splitting of the 16-electron 1,3-dipole as the key factor that determines the trend of the activation barrier and the reaction enthalpy. In this study, we have shown that the singlet−triplet splitting in the 16-electron 1,3-dipoles strongly correlates with their chemical reactivity. Also, we have suggested that the electronegativity of the atomic substituents is an important, perhaps decisive, factor in determining the singlet−triplet splitting of the 16-electron 1,3-dipoles and related isoelectronic molecules. Despite its simplicity, our approach provides a deeper insight and promises a solution of remaining problems soon.

Additional investigations of cycloadditions with other 18-electron 1,3-dipoles and the substituent effects of other dipolarophiles on this chemistry are currently in progress.[51]

Note Added in Proof. After this manuscript was submitted, two independent investigations appeared: (a) Karadakov, P. B.; Cooper, D. L.; Gerratt, J. *Theor. Chim. Acta* **1998**, *100*, 222. (b) Nguyen, M. T.; Chandra, A. K.; Sakai, S.; Morokuma, K. *J. Org. Chem.* **1999**, *64*, 65. It is found that our theoretical results are in reasonably good agreement with their work.

JO990504J

(49) Su, M.-D. *Int. J. Quantum Chem.* **1993**, *48*, 249.
(50) It is of interest to note that the cycloaddition of nitrile imine (**CNN**) is more favorable than that of diazomethane (**NNC**) as given in Table 2. The reason for this can also be traced back to the singlet−triplet splitting of these 1,3-dipoles. See Table 3.

(51) Liao, H.-Y.; Su, M.-D.; Chung, W.-S.; Chu, S.-Y., unpublished work.